Dynamics of the binary asteroid system (22) Kalliope-Linus based on observations

N. V. Emelyanov, B. S. Safonov, C. D. Kupreeva

Monthly Notices
of the
ROYAL ASTRONOMICAL SOCIETY

MNRAS **489,** 3953–3965 (2019) doi:10.1093/mnras/stz2411

Dynamics of the binary asteroid system (22) Kalliope–Linus based on observations

N. V. Emelyanov,[1,2]★ B. S. Safonov[1] and C. D. Kupreeva[3]

[1]*M. V. Lomonosov Moscow State University – Sternberg Astronomical Institute, 13 Universitetskij Prospect, 119234 Moscow, Russia*
[2]*Institut de mécanique céleste et de calcul des éphémérides – Observatoire de Paris, UMR 8028 du CNRS, 77 avenue Denfert-Rochereau, 75014 Paris, France*
[3]*M. V. Lomonosov Moscow State University – Faculty of Physics, 1–2 Leninskie Gory, 119991 Moscow, Russia*

Accepted 2019 August 22. Received 2019 August 19; in original form 2019 March 20

ABSTRACT

The aim of this article is to determine the dynamical parameters of the asteroid (22) Kalliope with its satellite Linus, based on astrometric observations of this system. We use a model of the motion taking into account the gravitational influence of the primary's axisymmetric non-sphericity. This factor leads to precession of the line of apsides of the satellite, as well as precession of its orbit around the primary's axis of symmetry. The axisymmetric gravitational field of the primary is formed by the time-averaged field of the fast-rotating body of Kalliope. All available observations of the Kalliope–Linus system were divided into groups, each containing observations close in time. For each group, parameters of the fixed Keplerian orbit were determined. Thus, the behaviour of the satellite's orbit axis over about 16-yr time intervals was studied. Contrary to the expected uniform precession of the orbital plane, we discovered abnormal prograde motion of the ascending node in the first seven years, which became retrograde in the next nine years. The amplitude of the change is about 120°. We make an attempt to explain such motion by effects not taken into account in the adopted dynamical model. It is shown that effects not taken into account cannot explain the oscillatory motion of the orbital node found. Using 121 available observations, two formal solutions for all fitted parameters were determined.

Key words: astrometry – celestial mechanics – minor planets, asteroids: general – minor planets, asteroids: individual: Kalliope.

1 INTRODUCTION

Satellites of asteroids are quite remarkable objects of the Solar system. Their study is useful for solving many practical problems related to planets and satellites. Slightly more than 300 asteroids are known to have satellites. In most cases, however, the only thing known is that an asteroid does have a satellite. There are only about 50 asteroids for which enough observations are available to determine satellite orbits.

The study of orbital dynamics of asteroid satellites is necessary primarily for determination of the mass of an asteroid system. Lack of data about the masses of asteroids is one of the reasons why models of planetary motions still have limited precision. A more detailed study based on a sufficient number of observations will provide us with information about the dynamical parameters of orbits of both the primary and the satellite.

There are two ways of getting information about asteroids with satellites. The first one is to observe the visual shapes of bodies. This is done either by using photographs made by spacecraft or by carrying out Earth-based photometric observations of mutual occultations and eclipses by the satellite and the primary or observing occultations of stars by asteroids. These methods give information about the visual shape of the primary and its orientation in space. No information, however, can be acquired about what is inside the body of the asteroid.

To determine the gravitational field parameters of the primary's body, it is necessary to study the orbital dynamics of satellites. It is not obvious that information about the visual shape and orientation of the primary will coincide with the results of study of the primary's gravitational field. Comparing data obtained in different ways can result in interesting interpretations.

The dynamics of an asteroid's satellites and dynamical properties of the primary can be studied using positional observations of satellites. The motion of the satellites is also dependent upon the orientation and rotation of the primary, which creates a gravitational field for the satellites. That is why the dynamical behaviour of the primary should be studied along with the satellite orbital dynamics.

Since there are only rare cases in which photographs with known scales and orientations were made by space missions, we leave such observations outside our consideration.

★ E-mail: emelia@sai.msu.ru

Thus, there are only two means of Earth-based observation from which positional data can be obtained: direct imaging of asteroids with satellites and photometric observations of asteroid systems during mutual occultations and eclipses. Two factors interfere with obtaining the images. The first one is the extreme visual proximity of the two objects, with the angular distances between satellites and primary not exceeding one arcsec. The second factor is the large image contrasts, i.e. the great differences in magnitude of the primary and its satellites. To overcome these obstacles, new observational methods are used: speckle interferometry and adaptive optics. These tools improve image quality and permit us to obtain more precise positional measurements. As for obtaining positional data from photometric observations of mutual occultations and eclipses, solving this problem is difficult, due to uncertainties in our knowledge of the shapes of the objects in question. Both non-sphericity of rotating asteroids and mutual occultations and eclipses result in roughly the same amount of fluctuations in the total brightness of the system, so that it becomes difficult or even impossible to distinguish between these two effects. Thus, it is necessary to obtain, from photometry, positional data together with body shape parameters.

New positional observations of asteroid satellites are obtained very rarely. This is why both the results of observations and the values of fitted dynamical parameters are usually published together in the same articles. As a result, observations are scattered in different articles. Note, however, that a complete and regularly updated database of all astrometric observations of asteroid satellites has been launched recently (Emel'yanov, Vashkov'yak & Ural'skaya 2018). The database is available at http://www.sai.msu.ru/neb/nss/html/obspos/babine.htm.

Models of satellite motion can take into account the gravitational influence of oblateness or the extension of the axisymmetric gravitational field of the system's primary. These factors result in precession of the line of apsides and precession of the satellite's orbit around an asteroid having an axisymmetric gravitational field. To observe this effect, it is necessary for the orbit to turn significantly. Only then is it possible to determine the oblateness and axis orientation of the primary. Obviously, progress in this issue can be achieved only by carrying out new observations.

Our choice fell on the system of asteroid (22) Kalliope and its satellite Linus. Taking into consideration the above, we used a series of new positional speckle interferometry observations of the Kalliope–Linus system made in 2017–2018 with the telescope of the Caucasian Mountain Observatory (CMO) of the Sternberg Astronomical Institute (SAI), Moscow State University (MSU). These observations extended the interval of observations from 10.3 to 16.7 years. This, in turn, provided an opportunity to determine all the parameters of the satellite's orbit, the mass of the system, Kalliope's oblateness and the coordinates of its pole.

Such results would permit us, for the first time, to evaluate the dynamical effect of the asteroid's oblateness, while the results of earlier studies were based on photometric observations and provided only the external visual shape of Kalliope, which did not necessarily reflect its gravitational field.

This is the outline of our work. Below we describe the methods used and the results.

2 THE DYNAMICAL MODEL

Before fitting parameters to observations, it is necessary to adopt a model of the dynamical system, i.e. the properties of its objects and a model of the forces in action. To simplify further presentation, we shall call the primary a planet. This is quite acceptable, since asteroids are considered as minor planets of the Solar system.

Thus, we consider a planet with satellites. The planet can have a prolate or oblate body, the satellites being considered point objects.

In this study, we neglect mutual gravitational attraction between asteroid satellites. If an asteroid has more than one satellite, the motion of each of them can be considered independently. The attraction of the Sun and major planets is also neglected.

In the general case, the planet rotates and the axis of its rotation can change its position both in space and in the body of the planet. One option for the behaviour of the rotation axis is its permanent coincidence with the axis of the planet's gravitational field symmetry. If it also happens that the satellite is moving in the plane coinciding with that of the planet's equator, then there is no reason in this hypothetical model for precession of either the satellite's orbit or the rotation axis. Otherwise, axes do have precession.

Neglecting short-period perturbations, we assume the orbit of the satellite to be planar, the orbital plane precessing around some axis. We call the line normal to the orbital plane the orbital axis.

As is well known, there are instances in the Solar system where the rotation axis of the planet is precessing synchronously with the precession of the satellite's orbital plane around a fixed vector of the total angular momentum. The precession of the orbit is caused by the influence of dynamical oblateness or extension of the planet. Synchronous precession appears due to tidal evolution. Instances of such systems are Earth–Moon and Neptune–Triton.

In our model, we assume that the orbital plane is precessing with a constant inclination around some fixed axis, which we call the precession axis. The angular coordinates of this axis, inclination of the orbit and precession rate are to be determined from observations.

The planet's rotation axis can be different from its precession axis. We assume, however, that the rotation axis coincides with the axis of symmetry of the planet's gravitational field. We also assume that the rotation axis precesses with constant inclination to the fixed precession axis, synchronously with the precession of the satellite's orbit. According to the conservation law for angular momentum, all the three axes should lie in the same plane. Inclinations of axes to the precession axis are supposed to be less than 90°. The northern direction of the axes is chosen in such a way that the satellite has direct motion along its orbit.

In the general case, the body of the planet has an arbitrary shape. However, if it rotates sufficiently quickly compared with the orbital motion of the satellite, the time-averaged gravitational field strength will affect the motion of the satellite in roughly the same way as if the planet's gravitational field had axial symmetry, with the symmetry axis coinciding with the rotation axis. This is the assumption made in our model.

In the reference frame related to the planet's equator, the potential function of an axisymmetric planet field can be expanded in a series of spherical harmonics. In this expansion, we leave only the main term and the second zonal harmonics. The corresponding coefficient J_2 characterizes the dynamical oblateness or extension of the planet.

Our assumption about synchronous precession of the axes should be confirmed by observations. In this study, we will determine orbital precession on the basis of astrometric observations of satellites. Data on precession of the planet's rotation axis are to be found in other articles.

3 TYPES OF OBSERVATIONS

Let us now consider the types of observations we use. The results of positional observations are usually differences of geoequatorial coordinates of the satellite and planet. In this case, the difference of right ascensions is multiplied by the cosine of declination of the planet. This is necessary for the errors of observations obtained for different declinations to make equal contributions to the errors of the parameters to be determined. Let us designate the values to be measured as follows:

$$X^{\rm o} = (\alpha_{\rm s} - \alpha_{\rm p})\cos\delta_{\rm p}, \qquad Y^{\rm o} = (\delta_{\rm s} - \delta_{\rm p}),$$

where $\alpha_{\rm s}$ and $\delta_{\rm s}$ are the right ascension and declination of the satellite; $\alpha_{\rm p}$ and $\delta_{\rm p}$ are those of the planet. In practice, the apparent angular distance s and position angle P are also used; they are related to the above parameters by the formulae

$$s = \sqrt{X^{\rm o2} + Y^{\rm o2}}, \qquad \tan P = \frac{X^{\rm o}}{Y^{\rm o}}. \tag{1}$$

Note that the same letters, X and Y, are often used for the rectangular heliocentric coordinates of asteroids. To distinguish between these two designations, it is necessary to take notice of the indices of these values.

Positional data can be extracted from photometric observations of asteroids during their mutual occultations and eclipses with the satellite. However, we did not use such observations in our study.

4 THE MODEL OF SATELLITE MOTION AND PARAMETERS TO BE DETERMINED

We used the dynamical model described above in our study. In this model, the unknowns are the orbital parameters of the satellite, the total mass of the planet and satellite, the coefficient J_2 and the angles of orientation of the planet's gravitational field axis of symmetry.

The main perturbing factor in our problem is the non-sphericity of the axisymmetric planet's gravitational field. Thus, to take perturbations into account, it is convenient to relate the main reference frame to the planet's equatorial plane normal to the axis of gravitational field symmetry. We denote coordinates in this frame as $\overline{x}$, $\overline{y}$ and $\overline{z}$. The axis $\overline{z}$ is directed along the axis of symmetry of the planet's gravitational field.

Directions of the axes $\overline{x}$ and $\overline{y}$ are chosen in the way described below.

Observations give us relative coordinates of the satellite in the geoequatorial reference frame, the axes of which we designate as x, y, z. It is necessary to find the relationship between $\overline{x}$, $\overline{y}$, $\overline{z}$ and x, y, z. Let the axis $\overline{x}$ be directed towards the ascending node of the plane $\overline{x}$, $\overline{y}$ over the plane x, y. Then the relationship between two reference frames is given by the formula:

$$\{x, y, z\}^{\rm T} = \mathbf{S}_0\{\overline{x}, \overline{y}, \overline{z}\}^{\rm T}, \tag{2}$$

where

$$\mathbf{S}_0 = \begin{pmatrix} -\sin\alpha_0 & -\cos\alpha_0\sin\delta_0 & \cos\alpha_0\cos\delta_0 \\ \cos\alpha_0 & -\sin\alpha_0\sin\delta_0 & \sin\alpha_0\cos\delta_0 \\ 0 & \cos\delta_0 & \sin\delta_0 \end{pmatrix}$$

and α_0, δ_0 are the right ascension and declination of the planet's northern pole.

Since, in our problem, the planet is assumed to be axisymmetric, it does not matter which direction of the symmetry axis is taken as the northern one. However, for definiteness, we use the rule adopted for small bodies of the Solar system (Archinal et al. 2018), according to which the north pole is that directed along the vector of the planet's angular rotation.

The motion of the satellite is described by differential equations of motion expressed in the coordinates $\overline{x}$, $\overline{y}$, $\overline{z}$:

$$\frac{{\rm d}\overline{x}}{{\rm d}t} = -Gm\frac{\overline{x}}{r^3} + \frac{\partial R}{\partial \overline{x}},$$

$$\frac{{\rm d}\overline{y}}{{\rm d}t} = -Gm\frac{\overline{y}}{r^3} + \frac{\partial R}{\partial \overline{y}},$$

$$\frac{{\rm d}\overline{z}}{{\rm d}t} = -Gm\frac{\overline{z}}{r^3} + \frac{\partial R}{\partial \overline{z}},$$

where, according to the adopted dynamical model, the perturbing function

$$R = -GmJ_2\frac{r_0^2}{r^2}\left(\frac{3}{2}\frac{\overline{z}^2}{r^2} - \frac{1}{2}\right) \tag{3}$$

describes the influence of the second zonal harmonics in the expansion of the planet's potential function. The following notation is also used: r_0 is the mean radius of the planet; G, the universal gravitational constant; m, the total mass of the planet and satellite,

$$r = \sqrt{\overline{x}^2 + \overline{y}^2 + \overline{z}^2}.$$

The sign of the perturbing function in (3) is chosen in such a way that $J_2 > 0$ for an oblate planet and $J_2 < 0$ for a prolate one.

The model of the satellite's perturbing motion can be built by solving the differential equations of motion using methods from the theory of perturbations. It is known that there are no long-term perturbations caused by the second zonal harmonics. The short-period terms are small and can be neglected. Hence only secular terms remain and the model of the satellite's motion can be reduced to that of a precessing ellipse. In this case, the elements of a Keplerian orbit, the mean anomaly M, the argument of pericentre ω and the longitude of the ascending node Ω, are represented with linear functions of time:

$$M = M_0 + \overline{n}(t - t_0),$$

$$\omega = \omega_0 + \dot{\omega}(t - t_0),$$

$$\Omega = \Omega_0 + \dot{\Omega}(t - t_0), \tag{4}$$

where $\overline{n}$ is the perturbed value of the mean motion, t is the time and t_0 the epoch.

In the formulae of Keplerian motion, the perturbed value $\overline{a}$ should be used as the value of the semimajor axis a. The other two elements, inclination i and eccentricity e, are constant. According to the theory of perturbations, the secular rates $\dot{\omega}$ and $\dot{\Omega}$ and the perturbed value of the mean motion $\overline{n}$ are given by the formulae

$$\overline{n} = n + \frac{3}{4}nJ_2\left(\frac{r_0}{a}\right)^2\frac{2 - 3\sin^2 i}{(1 - e^2)^{3/2}},$$

$$\dot{\omega} = \frac{3}{4}nJ_2\left(\frac{r_0}{a}\right)^2\frac{4 - 5\sin^2 i}{(1 - e^2)^2},$$

$$\dot{\Omega} = -\frac{3}{2}nJ_2\left(\frac{r_0}{a}\right)^2\frac{\cos i}{(1 - e^2)^2}, \tag{5}$$

where n is the unperturbed mean motion. For secular perturbations, only the terms of first order as regards the coefficient J_2 are taken into account.

The set of formulae for our computations is completed with the following relation for the perturbed semimajor axis:

$$\overline{a} = a\left[1 - \frac{3}{4}J_2\frac{r_0^2}{a^2}(2 - 3\sin^2 i)\right]. \quad (6)$$

This expression is approximate, because the eccentricity, which is much lower than unity, is neglected.

Now it is possible to provide the formula for the mass of the system obtained from the perturbed $\overline{a}$ and $\overline{n}$ fitted to observations:

$$\overline{a}^3\overline{n}^2 = Gm\left[1 - \frac{3}{4}J_2\frac{r_0^2}{a^2}(2 - 3\sin^2 i)\right]. \quad (7)$$

Here, eccentricity is also neglected.

Obviously, it is from positional observations of a satellite that precession of its orbit can be detected. Such precession is caused by dynamical non-sphericity of the planet. However, if there is no precession, it is not possible to derive its axis from observations. There are two reasons why precession may be absent. The first one is that the planet's non-sphericity can be too small, so that the coefficient J_2 is negligible. The second possible reason is that the time interval of observations may be too short, so that the turn of the orbital plane is so small that it is impossible to find out around which axis rotation occurs. For these reasons, it may be impossible to find the orientation of the planet's axis, i.e. the parameters α_0 and δ_0, from observations. Then, the coefficient J_2 cannot be determined either. In such circumstances, the planet's axis orientation is fixed arbitrarily and an attempt is made to fit the remaining parameters to observations. The simplest choice is to assume that the two reference frames, $\overline{x}$, $\overline{y}$, $\overline{z}$ and x, y, z, coincide, that is, to take $\alpha_0 = -90^\circ$ and $\delta_0 = 90^\circ$.

Thus, let us list the parameters to be determined from observations.

First, we consider the case when the asteroid has only one satellite. Then, the following independent parameters can be derived:

$\alpha_0, \delta_0, J_2, \overline{a}, \overline{n}, e, i, M_0, \omega_0, \Omega_0$.

Having determined these parameters, we can find the total mass of the system from (7). If precession is small, the parameters α_0, δ_0, J_2 drop out from the list. The mass of the system in this case can be determined only approximately, either by putting $J_2 = 0$ or by adopting some hypothetical value for this coefficient.

The second case is when the asteroid has two satellites. Then, the parameters α_0, δ_0, J_2 will be common for both satellites. Instead of perturbed values of semimajor axes, the gravitational parameter common for the two satellites,

$\mu = Gm$,

needs to be determined.

5 THE METHOD OF FITTING PARAMETERS TO OBSERVATIONS

To fit the parameters to observations, differential correction, along with the least-squares method, was used. Below we give a short description of this methodology.

In the general case, we have a set of parameters to be determined: $p_1, p_2, ..., p_n$ and the measured values ξ. As a result of observations, for each time t_i ($i = 1, 2, 3, ..., m$), we have a measured value. Then, conditional equations can be written:

$$\xi_i^{\rm o} = \xi(t_i, p_1, p_2, ..., p_n) \qquad (i = 1, 2, 3, ..., m), \quad (8)$$

where the function $\xi(t_i, p_1, p_2, ..., p_n)$ is called the model of motion.

The system (8) is inconsistent: that is, it has no solution. Hence, we can only try to get estimated values of the unknown parameters using some appropriate method.

First, we build a system of linear conditional equations. Suppose that someone has already tried to determine the parameters in question and found their approximate values. We denote such preliminary values as $p_1^{(0)}, p_2^{(0)}, ..., p_n^{(0)}$.

Let the difference between precise values of the parameters p_1, p_2, ..., p_n and preliminary ones be

$$\Delta p_1 = p_1 - p_1^{(0)}, \quad \Delta p_2 = p_2 - p_2^{(0)}, \ \dots, \ \Delta p_n = p_n - p_n^{(0)}.$$

Then, (8) can be written as

$$\xi_i^{\rm o} = \xi(t_i, p_1^{(0)} + \Delta p_1, p_2^{(0)} + \Delta p_2, \dots, p_n^{(0)} + \Delta p_n). \quad (9)$$

The preliminary values are close enough to the precise ones to allow us to consider the corrections $\Delta p_1, \Delta p_2, \dots, \Delta p_n$ to be small and expand the right-hand side of (9) into a Taylor series in powers of these corrections:

$$\xi_i^{\rm o} = \xi(t_i, p_1^{(0)}, p_2^{(0)}, \dots, p_n^{(0)}) + \sum_{k=1}^{n}\left(\frac{\partial\xi}{\partial p_k}\right)_i \Delta p_k + \ \dots .$$

The derivatives on the right-hand sides of the equations are calculated by putting

$t = t_i, \quad p_1 = p_1^{(0)}, \ \dots, \ p_n = p_n^{(0)}$.

Leaving only the first-order terms with respect to Δp_k, we introduce the following notations:

$$\xi_i^{\rm c(0)} = \xi(t_i, p_1^{(0)}, p_2^{(0)}, \dots, p_n^{(0)}), \quad (10)$$

$$a_k^{(i)} = \left(\frac{\partial\xi}{\partial p_k}\right)_i, \quad (11)$$

$$\Delta\xi_i = \xi_i^{\rm o} - \xi_i^{\rm c(0)}.$$

As a result, we obtain

$$\Delta\xi_i = \sum_{k=1}^{n} a_k^{(i)}\Delta p_k, \quad (i = 1, 2, \dots, m). \quad (12)$$

The approximate relations (12) are called *conditional equations* for finding corrections to the fitted parameters. These are linear inhomogeneous algebraic equations for the required corrections $\Delta p_k \quad (k = 1, 2, \dots, n)$.

Making assumptions about the errors of the theory and observations, one of the methods to find an approximate solution of the conditional equations in (12) can be chosen. The existing methods also make it possible to evaluate the errors of the solution.

Having found the corrections, we add them to the preliminary values and obtain new and, hopefully, more precise parameters. It is this method of finding the parameters of motion of celestial bodies that is called *differential correction*.

Since the conditional equations and their solutions are approximate, the new parameters will not be precise enough. However, fitting the parameters can be repeated several times. If the process converges, that is, corrections decrease with each iteration, calculations can be stopped when the corrections become sufficiently smaller than their errors. In this case, we obtain the parameters $\overline{p}_1, \overline{p}_2, ..., \overline{p}_n$ corresponding to all observations that were used. This correspondence is determined uniquely by the adopted model of motion and the algorithm chosen to obtain the estimated parameters.

The algorithm we use is the least-squares method, the reason for its choice being its simplicity. According to this method, on the base of the conditional equations, the system of normal equations, which is a system of n linear inhomogeneous equations, is composed.

Observations are often given along with the estimated error of each observation. In such a case, appropriate weights can be assigned to each conditional equation.

It appears from the above formulae that, in order to fit the parameters, it is first necessary to compose the conditional equations. For this, the function (10) and its partial derivatives (11) should be calculated for each date of observations. The measured values $X^{\rm o}$ and $Y^{\rm o}$ depend on the asteroid's topocentric geoequatorial coordinates X, Y, Z and on the satellite's planetocentric geoequatorial coordinates x, y, z, that is:

$$X^{\rm o} = X^{\rm o}(X, Y, Z, x, y, z), \qquad Y^{\rm o} = Y^{\rm o}(X, Y, Z, x, y, z).$$

The formulae necessary for their calculations are taken from Emelianov (1999). Here, we have

$$X = X^{\rm a} - X^{\rm T}, \qquad Y = Y^{\rm a} - Y^{\rm T}, \qquad Z = Z^{\rm a} - Z^{\rm T}, \tag{13}$$

where $X^{\rm T}$, $Y^{\rm T}$, $Z^{\rm T}$ are the heliocentric coordinates of the topocentre calculated for the date of observation t_i and $X^{\rm a}$, $Y^{\rm a}$, $Z^{\rm a}$ are the heliocentric coordinates of the asteroid calculated for the date $t_i - \Delta t_i$, where Δt_i is the light delay time. The planetocentric coordinates of the satellite should also be calculated for the same date.

The heliocentric coordinates of the topocentre $X^{\rm T}$, $Y^{\rm T}$, $Z^{\rm T}$ are calculated using the software and data provided with the planetary ephemeris INPOP17a (Viswanathan et al. 2017). The asteroid's heliocentric coordinates $X^{\rm a}$, $Y^{\rm a}$, $Z^{\rm a}$ are computed using our original calculating program EMEASTER, which models the motion of asteroids on the basis of their observations. For this, we take as observations the ephemerides of asteroids computed with the MIRIADE software elaborated in the Institut de mécanique céleste et de calcul des éphémérides (IMCCE), Paris, France (available at http://vo.imcce.fr/webservices/miriade/?forms).

The algorithms of EMEASTER take into account attraction by all the major planets and the Moon. Thus, sufficiently precise determination of heliocentric coordinates of asteroids is provided. At the beginning of its work, EMEASTER uses the ephemeris to refine the initial conditions of integration of the differential equations of an asteroid's motion. In the course of integration, arrays of coefficients for the segments of the Chebyshev series expansion for rectangular heliocentric coordinates are created. It is by using these segments of the Chebyshev series that, in refining the satellite's orbit, heliocentric coordinates of the asteroid are computed. To obtain topocentric coordinates, the coordinates of the observatory are added to the ephemeris coordinates of the geocentre.

In the case in which there are observations of only one satellite, the initial parameters for calculating the measured values are α_0, δ_0, J_2, $\overline{a}$, $\overline{n}$, e, i, M_0, ω_0, Ω_0. The following sequence of calculations is made.

For a given date of observation t_i, the values M, ω, Ω are computed using the formulae (4) and (5), where the value of J_2 is substituted. In (5), taking into account the adopted accuracy, the perturbed values $\overline{a}$ and $\overline{n}$ can be taken instead of a and n. Then, the values of $\overline{a}$, e, i, M, ω, Ω are substituted into the formulae of Keplerian motion and the satellite's planetocentric rectangular coordinates $\overline{x}$, $\overline{y}$, $\overline{z}$ referred to the planet's equator can be obtained. The satellite's planetoequatorial coordinates are then referred to the system of the Earth's equator by using the relations (2) with substituted values of α_0 and δ_0. After that, heliocentric coordinates of the topocentre and asteroid are computed in the manner described above. Finally, using (13) and the formulae given in Emelianov (1999), we find the measured values $X^{\rm o}$ and $Y^{\rm o}$.

If two satellites are observed, then, instead of pregiven values of the parameters $\overline{a}^{(1)}$, $\overline{a}^{(2)}$, only one parameter μ is given. The perturbed semimajor axes are obtained from the relation

$$\overline{a}^3 = \frac{\mu}{\overline{n}^2}\left[1 - \frac{3}{4}J_2\frac{r_0^2}{a^2}(2 - 3\sin^2 i)\right],$$

where a is computed by iterations using the formula (6).

After the parameters are determined, the so-called root-mean-square (rms) residual σ is computed, which shows the agreement of observations with theory. To obtain it, for each date of observation with index i, the values $\delta X_i = X_i^{\rm o} - X_i^{\rm c}$ and $\delta Y_i = Y_i^{\rm o} - Y_i^{\rm c}$ are calculated, where $X_i^{\rm o}$ and $Y_i^{\rm o}$ are the measured values obtained from observations in the manner described above; $X_i^{\rm c}$ and $Y_i^{\rm c}$ are the same values obtained from the satellite's model of motion. The residual σ is defined by

$$\sigma = \sqrt{\frac{1}{2m}\sum_{j=1}^{m}\left[(\delta X_i)^2 + (\delta Y_i)^2\right]}, \tag{14}$$

where m is the number of observations (positions) of the satellite. Besides the rms residual determined in this way, the weighted rms residual $\sigma_{\rm w}$ is also calculated.

6 THE CHOICE OF THE OBJECT AND NEW OBSERVATIONS

Among those asteroids that possess satellites, only a few have more than six observations. However, to find orbital parameters, more observations are necessary, which should be carried out over as long an interval as possible. Even if it is possible to determine the orbit, the orientation of the symmetry axis and oblateness of the primary are not always guaranteed. As explained earlier, it is necessary for this determination that the precession be significant over the time interval of observations.

To choose objects for our study, we used the database of observations of asteroid satellites ABIN (Emel'yanov et al. 2018). By an observation, we mean the relative position of the satellite at some time. At the first glance, from the point of view of numbers of observations and time intervals, the most appropriate objects to study are the following four systems.

1 The system of the asteroid 22 Kalliope with the satellite Linus. There are 121 observations over a 16.7-yr time interval.

2 The system of the asteroid 87 Sylvia with the satellites Remus (45 observations) and Romulus (112 observations). Observations of both satellites cover a 10-yr time interval.

3 The system of the asteroid 45 Eugenia with the satellites Princesse and Petit-Prince. The time interval of observations is 7 years.

4 The system of the asteroid 136108 with the satellites Hi'iaka and Namaka. The time interval of observations is 3 years.

After attempts to determine the parameters for these objects, the following was found. In the system of (136108) Haumea, mutual gravitational perturbations between satellites are strong. Such perturbations cannot be taken into account in our dynamical model and algorithm for determination of the parameters. Hence, our model cannot be applied to this system. In the systems of 45 Eugenia and 87 Sylvia, the orbital precession turned out to be so small that it was not possible to determine the coordinates of the symmetry axis of the primary.

Table 1. Observations of Kalliope's satellite Linus. The following notation is used: JD is the Julian date of observation (UTC); s, the angular distance (mas); σ_s, the error of the angular distance (mas); P, the position angle (°); σ_P the error of the position angle (°).

JD	s	σ_s	P	σ_P
2458090.62349	479	2	289	1
2458091.60310	469	2	191	1
2458091.62832	473	1	190	1
2458091.63624	462	1	191	1
2458100.62637	476	1	8	1
2458100.65069	480	1	7	1
2458100.65676	473	2	7	1
2458147.64806	543	1	338	1
2458156.61001	585	2	162	1
2458177.44177	654	2	238	1
2458177.52959	636	3	228	1
2458177.57168	652	2	223	1
2458180.47423	706	2	295	1
2458180.53804	665	5	290	1
2458180.54302	628	5	286	1
2458180.59594	675	2	281	1
2458183.57010	689	3	342	1
2458210.31971	663	5	184	1
2458214.41011	670	5	133	1
2458215.37401	660	5	37	1
2458216.42677	683	5	293	1
2458217.25499	662	5	212	1
2458218.28200	692	5	106	1
2458233.26260	673	5	48	1
2458234.34748	666	5	298	1
2458238.32053	656	6	261	1
2458255.30038	618	5	1	1
2458264.28622	577	5	181	1

Thus, our choice for the study fell on the system of 22 Kalliope and Linus. It was all the more favourable a case for the study, as new observations of Linus had been carried out by B. S. Safonov (SAI MSU) which extended the time interval of observations from 10.3 to 16.7 years. The new data are 28 positions of Linus relative to Kalliope in the interval between 2017 December 3 and 2018 May 26. The coordinates are the angular distances and position angles (see Section 3).

The observations were carried out using a speckle polarimeter, a facility instrument of the 2.5-m telescope of CMO of SAI MSU (Safonov, Lysenko & Dodin 2017). The speckle polarimeter is a combination of a dual-beam polarimeter and a speckle interferometer. The detector used in the instrument is a fast electron-multiplying CCD Andor iXon 897. The detector has a size of 512 × 512 pixels, the estimated scale being about 20.6 mas per pixel.

Two orthogonally polarized images of the object are imaged on the detector side by side. The resulting effective field of view is 5 × 10 arcsec^2 Since polarization of the object does not interest us in this study, the power spectra corresponding to orthogonal polarizations are simply averaged. Typical exposures are from 30–60 ms, typical numbers of accumulated frames are from 5000–8000. Processing was made by the standard speckle interferometry method; the details are given in Safonov et al. (2017). To define the scale and positional angle of the detector, observations of several binary stars separated by 3–5 arcsec were made. The results of the new observations are given in Table 1.

To determine the dynamical parameters of the Kalliope–Linus system, all observations of the satellite available in the database ABIN (Emel'yanov et al. 2018) were used, along with the new observations. In total, 121 relative positions of the satellite were used.

Table 2. The observations used in this article. The following notation is used: ABIN is the index of the portion in the ABIN database, N is the number of satellite positions taken in this portion.

ABIN	Dates of observations (from–to), year, month, day	N	References
0049	2001.08.29–2001.08.29	1(9)	(Margot & Brown 2003)
0074	2001.09.02–2001.09.03	3	(Merline et al. 2001)
0012	2001.10.03–2001.11.03	15	(Marchis et al. 2003)
0015	2001.08.31–2006 12 12	46	(Marchis et al. 2008)
0106	2006.11.07–2006.11.07	1	(Soma et al. 2008)
0013	2007.03.08–2007.03.17	4	(Descamps et al. 2008)
0134	2010.06.28–2010.09.17	15	(Vachier et al. 2012)
0027	2011.12.10–2011.12.16	8	(Sokova et al. 2014)
0135	2017.12.03–2018.05.26	28	This paper (Table 1)

Table 2 presents the obsevations with references to their publications. Note that only one position was taken from the portion 0049 (2001/08/29), whereas the other eight were taken from the portion 0015.

7 RESULTS OF THE DETERMINATION OF DYNAMICAL PARAMETERS OF THE KALLIOPE–LINUS SYSTEM

Thus, we attempt to fit the dynamical parameters of the Kalliope–Linus system to all available observations. As mentioned above, 121 observations of the satellite's relative position made between 2001 August 29 and 2018 May 26, about a 16.7-yr time interval, were used.

Our main aim was to fit all 10 parameters, including the coordinates of the pole of precession, α_0 and δ_0, and Kalliope's oblateness coefficient J_2, to all observations. According to the adopted dynamical model, this would result in uniform rotation of the orbit's pole around the pole of precession, the angular rate of this rotation being equal to that of the ascending node Ω defined by (5).

Precession of the pole of the satellite's orbit depends on the position of the symmetry axis of the body causing the precession, which, in our case, is the fast-rotating body of Kalliope. The gravitational field averaged over time will have the same effect as the field of some axisymmetric body. In this case, the symmetry axis will coincide with the rotation axis. The position of Kalliope's rotation axis, found from photometric observations, was published by Descamps et al. (2008), where three variants of the coordinates of the rotation axis are given. These coordinates may also be found in the database of asteroid models DAMIT (Durech, Sidorin & Kaasalainen 2010).

If we suppose that Kalliope rotates around the axis coinciding with the vector of maximum moment of inertia, the time-averaged gravitational field would correspond to an oblate body with $J_2 > 0$. In this case, the pole should constantly move in the direction opposite to that of the satellite's orbital motion with constant inclination to some fixed axis. The fixed axis of orbital precession should lie close to the rotation axis of the primary or coincide with it.

We had an opportunity to establish in advance the fact of precession of the satellite's orbital axis around some axis. This can

Table 3. Characteristics of the groups of observations used to determine the coordinates of the pole of a fixed orbit for a series of dates. *N* is the number of the group; *N* obs, the number of observations in the group; Int, the time interval of observations in the group; P_{pr}, the accuracy of the coordinates of the pole; sigma, the residual for the group (defined by equation 14); *T* is the satellite's orbital period.

N	Mean date, year	*N* obs.	Int, days	P_{pr} °	sigma, arcsec	*a*, km	*e*	*T* day
1	2001.769	39	102.4	0.3	0.120	1066	0.0065	3.596
2	2003.979	25	918.0	0.7	0.022	1085	0.0069	3.596
3	2007.099	6	131.1	1.0	0.009	1070	0.0075	3.595
4	2010.660	15	80.2	0.7	0.008	1118	0.0023	3.595
5	2011.952	8	5.2	0.2	0.004	1060	0.0110	3.604
6	2018.157	28	174.9	3.3	0.022	1080	0.0015	3.595

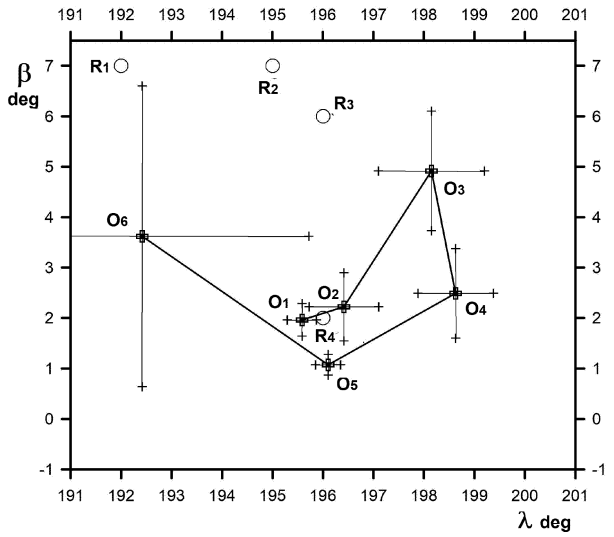

Figure 1. The ecliptic coordinates (λ, the longitude, and β, the latitude) of the orbit pole (the small crosses O_1, O_2, O_3, O_4, O_5, O_6) obtained from observations given for a series of dates (see Table 3). The circles R_1, R_2, R_3 show the positions of the rotation axis taken from Descamps et al. (2008), the circle R_4 corresponds to the position taken from Durech et al. (2010). The crossing lines at each point of the position of the orbit axis represent the error in determining the coordinates (1σ).

be done by determining the pole of a fixed orbit for a series of dates. To this end, all observations were divided into six groups, each group containing observations close in time. For each group, a fixed Keplerian orbit and its pole were determined. Characteristics of the groups of observations and obtained values of some parameters are given in Table 3.

In this analysis, some weights were assigned to each conditional equation using the estimated error of each observation. If the error was given with the observation, then this value was used, otherwise the estimated error was taken as the rms value of the differences of measured coordinates from calculated ones obtained during the iteration process.

A table containing all the astrometric data used in our solutions, along with the astrometric uncertainties, is provided with this article as Supplementary Material, available online. It is a snapshot of the exact values that were used for this analysis.

The coordinates of the orbit's pole obtained for each group were transformed into an ecliptic reference frame. The results are

Table 4. The formal solutions fitted to the whole set of 121 observations made in 2001.7–2018.4 (Solutions 1 and 2) and to 57 observations made in 2006.8–2018.4 (Solution 3). The inclination *i* is given in degrees, dΩ/d*t* and dω/d*t* are given in degrees per day. The values of σ are obtained from (14).

Parameter	Solution 1	Solution 2	Solution 3
λ_0, °	195.53 ± 0.41	197.61 ± 1.21	197.60 ± 1.88
β_0, °	3.39 ± 0.51	0.42 ± 0.92	5.09 ± 1.37
J_2	−0.034 ± 0.007	0.011 ± 0.016	0.021 ± 0.009
a, km	1074.8 ± 3.2	1074.8 ± 3.6	1076.6 ± 6.2
e	0.004 ± 0.002	0.002 ± 0.002	0.009 ± 0.002
Period, day	3.5957	3.5961	3.5965
Inclination *i*	1.86 ± 0.43	2.61 ± 1.01	2.40 ± 1.42
dΩ/d*t*	0.0363	−0.0116	−0.0225
dω/d*t*	−0.0726	0.0231	0.0450
σ, arcsec	0.029	0.027	0.031

presented in Fig. 1, where the sequence of points obtained for successive times proves that first there was prograde motion of the orbit's pole, which later turned to retrograde motion. It is also noticeable that the pole makes a kind of rotational motion around an axis close to Kalliope's axis of rotation, with inclination not exceeding 3°. Thus, it turns out that the motion of the pole does not correspond to the model of uniform orbital precession with constant inclination to the precession axis.

Note also that, if using only observations made in 2002–2003, the satellite's orbit is determined with low accuracy. Hence, these observations can only be used together with those with those made in 2004.

In each of the six determinations, the position of the orbit's pole depends heavily on which observations are used. Dropping one or two observations that have the worst agreement with the model results in significant changes in the coordinates of the orbit's pole found.

Next, we tried to determine all 10 fitted parameters, including the coordinates of the precession pole (α_0, δ_0) and the coefficient of Kalliope's oblateness (J_2), fitting them to the whole set of observations. The method for determining the dynamical parameters and the dynamical model of the system described above was used. Since the orbital axis behaviour described above does not correspond to the adopted dynamical model, the solution we are looking for can only be a formal one.

Two solutions were obtained, which are presented in Table 4 and in Figs 2 and 3. We computed all the parameters that might be necessary to obtain the satellite's ephemerides. However, since neither of the two solutions matches the found motion of the pole adequately, we do not give all the parameters, only those that are the most important. When new observations are made, it will be possible to compare the ephemerides with the observations using both solutions for the parameters.

As seen in Figs 2 and 3, neither of the formal solutions corresponds to the motion of the orbit pole determined using separate groups of observations.

In the first formal solution, all 10 parameters were fitted together. The fitting process converged quickly. However, in the second formal solution, a strong correlation appears between the mean motion *n* and the coefficient J_2, so that we had to fit these parameters one by one, together with other parameters.

It is necessary to note that it is the second solution that corresponds to the oblate body formed by the fast-rotating body of Kalliope.

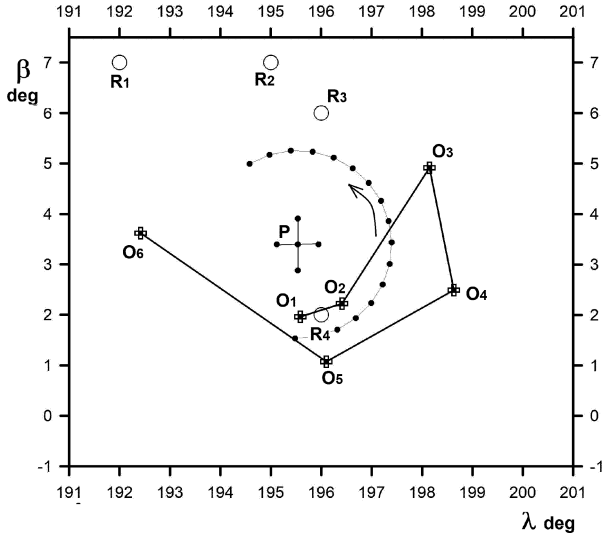

Figure 2. The ecliptic coordinates of the orbit pole (the dots connected by a line) computed for the interval from 2001–2017 using the formal solution 1. The cross in the middle is the position of the precession axis obtained and the error in determining the coordinates (1σ). The ecliptic coordinates of the orbit pole found from observations for a series of dates (see Table 3) are presented as crosses O_1, O_2, O_3, O_4, O_5, O_6. The circles R_1, R_2, R_3 are the positions of the rotation axis taken from Descamps et al. (2008), the circle R_4 is taken from Durech et al. (2010).

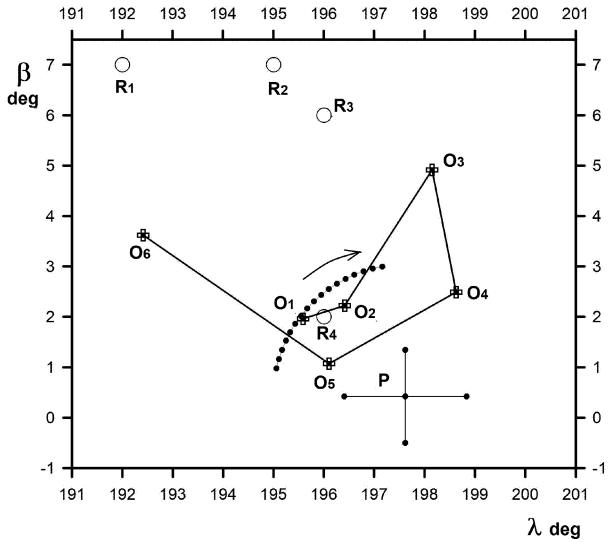

Figure 3. The ecliptic coordinates of the orbit pole (the dots connected by a line) computed for the interval from 2001–2017 using the formal solution 2. The cross in the middle is the position of the precession axis obtained and the error in determining the coordinates (1σ). The ecliptic coordinates of the orbit pole found from observations for a series of dates (see Table 3) are presented as crosses O_1, O_2, O_3, O_4, O_5, O_6. The circles R_1, R_2, R_3 are the positions of the rotation axis taken from Descamps et al. (2008), the circle R_4 is taken from Durech et al. (2010).

In 2006–2018, the orbit's pole was constantly rotating in the retrograde direction, which corresponds to $J_2 > 0$. For this time interval, all 10 fitted parameters were also determined using 57 observations. The result (solution 3) is presented in Fig. 4 and Table 4.

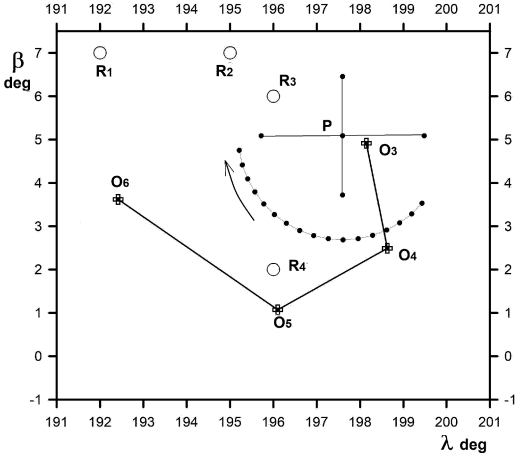

Figure 4. The ecliptic coordinates of the orbit pole (the dots connected by a line) computed for the interval from 2001–2017 using the formal solution 3. The cross in the middle is the position of the precession axis obtained and the error in determining the coordinates (1σ). The ecliptic coordinates of the orbit pole found from observations for a series of dates (see Table 3) are presented as crosses O_1, O_2, O_3, O_4, O_5, O_6. The circles R_1, R_2, R_3 are the positions of the rotation axis taken from Descamps et al. (2008), the circle R_4 is taken from Durech et al. (2010).

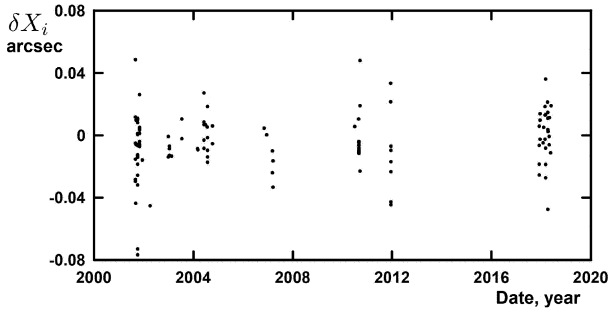

Figure 5. Residuals of observations in right ascension (O–C).

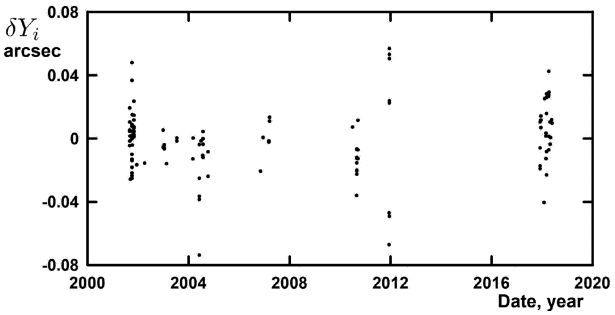

Figure 6. Residuals of observations in declination (O–C).

Both the solutions obtained by using groups of observations and the formal solutions fitted to the whole set of observations prove that the eccentricity of the orbit of Linus does not exceed 0.01.

Figs 5 and 6 display the residuals of each observation, for right ascension and declination, respectively, in solution 1.

To give an idea of what the observed angular distances between the satellite and the planet were, Fig. 7 displays, for each observation, the angular distance s_i determined from (1). The mean value of this distance over all the observations is 0.53 arcsec.

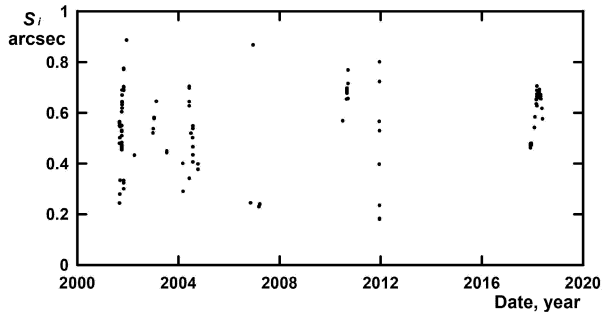

Figure 7. Angular distance between the satellite and the primary for each observation.

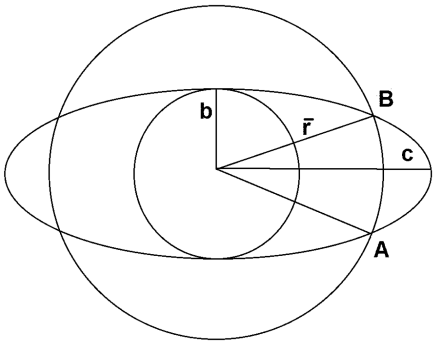

Figure 8. The scheme of mass distribution in a triaxial ellipsoid rotating around the minor axis a. The mass of the arc A–B is distributed over 180°.

8 THE GRAVITATIONAL FIELD PARAMETERS OF THE FAST-ROTATING BODY OF KALLIOPE

According to the adopted dynamical model of the orbital motion of an asteroid satellite, the primary is assumed to have axisymmetric mass distribution. In the Kalliope–Linus system, as has been found above, the period of the satellite orbital motion is approximately 3.596 days. At the same time, it can be concluded from Descamps et al. (2008) that the rotation period of Kalliope is 4.148 hours. Such a relation of the periods allows us to consider and adopt a model where the gravitational field of the primary is formed by the time-averaged gravitational field of the fast-rotating body of Kalliope. Since the real shape of Kalliope is not known exactly, we use a simplified model of a homogeneous triaxial ellipsoid. Descamps et al. (2008) give the approximate semiaxes of such a body: $a = 62.0$ km, $b = 82.0$ km, $c = 117.5$ km.

We assume that, in the process of its evolution, the rotation of Kalliope passed through the stage of tidal dissipation, which resulted in stable rotation around the minor axis $a = 62.0$ km. Thus, it is necessary to determine the parameters of the time-averaged gravitational field of such a rotating body. In rotating, some parts of the homogeneous triaxial ellipsoid can be considered as rigidly located in their places, while others become equivalent to a mass uniformly distributed along the circle centered around the axis a. Fig. 8 shows the mass distribution in the rotating triaxial ellipsoid schematically. It depicts a layer in the equatorial plane formed by the axes b and c, the ellipse being the projection of the ellipsoid's figure. In rotating, the mass of the arc between A and B is distributed along the 180° arc. The same happens with the arc on the opposite side of the ellipse. In other layers of the ellipsoid parallel to the equatorial plane, the mass distrubution is analogous.

We assume that the potential function U of the rotating body can be expanded in a series:

$$U = \frac{\mu_0}{r}\left[1 - \sum_{k=2}^{\infty} J_k \left(\frac{r_0}{r}\right)^k P_k(z/r)\right], \tag{15}$$

where μ_0 is the gravitational parameter of the body; r, the distance from the centre; z, the coordinate along the axis a; $P_k(...)$, the Legendre polynomials; r_0, the pregiven value of the body's mean radius; and J_k are the coefficients to be determined.

There is a problem of how to represent the products $r_0^k J_k$ analytically as functions of a, b and c. We leave this problem for future research, limiting ourselves to composing a computational program for numerical determination of these products.

For each k, the products we are looking for are given by the common formula

$$m_0 r_0^k J_k = -\int (r')^k P_k(z'/r')\rho' \, \mathrm{d}\tau',$$

where m_0 is the mass of the homogeneous triaxial ellipsoid with the axes a, b, c and the density ρ; τ', the volume element of the effective rotating body; z', r', the coordinate and central distance of the volume element; and ρ' the effective density of the volume element, i.e. the density ρ in those parts of the body that are rigidly located, while in other parts of the body it is a reduced density because of the rotation effect described above. Integration is carried out over the layers of the body parallel to the equator and along the radius $\bar{r}$ of the circle shown in the Fig. 8. Note that it is necessary to use the relation

$$r'^2 = \bar{r}^2 + z'^2.$$

There are reasons to suppose that the terms in (15) become smaller as n increases. That is why we confined ourselves to determining only the main terms in the expansion, those with the coefficients J_2 and J_4. After computation, we have $r_0^2 J_2 = 1284.21847$ and $r_0^4 J_4 = -4071488.42$. Assuming that $r_0 = 90$ km, we obtain $J_2 = 0.158545$ and $J_4 = -0.062056$.

Note that our computional program can obtain J_2 and J_4 for any values of a, b, c and r_0. Again, it is also of interest to derive analytical expressions for computing J_2 and J_4 as functions of the initial parameters.

9 ANALYSIS AND ESTIMATION OF PERTURBATIONS UNACCOUNTED FOR IN THE DYNAMICAL MODEL

Calculations of the satellite's orbit based on observations grouped in time intervals reveal a motion of the orbit pole not corresponding to the adopted dynamical model. In our model, the Keplerian motion is subject to perturbations caused only by J_2 terms in the expansion of the primary's potential function. It is quite reasonable to estimate the effects of those perturbations not taken into account. This section deals with such estimations.

In our dynamical model of the asteroid–satellite system, we neglected the attraction from the Sun, non-J_2 terms in the expansion of the potential function and non-sphericity of the satellite. Let us consider these effects one by one.

In estimating solar perturbations, the Sun is assumed to be an attracting body moving around the primary. The orbit of the Sun is a reflection of that of Kalliope, which can be considered as a fixed ellipse.

In our analysis, the following notation is used. Let μ' be the gravitational parameter of the Sun. For the elements of the orbit,

the same notation as for the satellite orbit is used, but with primes. In particular, we denote the semimajor axis of the Sun's orbit by a', the mean motion by n' and the eccentricity by e'. The elements i', ω', Ω' are referred to the ecliptic coordinate system.

The parameters of the Sun's orbit are those of Kalliope's orbit around the Sun with the argument of pericentre increased by 180°.

The elements in the ecliptic coordinate system are taken from the Minor Planet Center website. Thus, we take $a' = 2.909\,6538$ au, $n' = 0.198\,583\,01$ deg day^{-1}, $e' = 0.099\,2031$, $i' = 13.716\,68°$, $\omega' = 174.914\,34°$, $\Omega' = 66.066\,48°$.

Perturbations in the elements of the satellite orbit can be determined by the method of the theory of perturbations. We use the formulae given in Murray & Dermott (2000). Thus, for the first-order secular perturbations due to the Sun, we have

$$\frac{\mathrm{d}\omega}{\mathrm{d}t} = \gamma n \frac{3}{32} \frac{(3\sin^2 i' - 2)(2 + 3e'^2)}{\sqrt{1-e^2}} (5\sin^2 i - 4 - e^2),$$

$$\frac{\mathrm{d}\Omega}{\mathrm{d}t} = \gamma n \frac{3}{32} \frac{\cos i}{\sqrt{1-e^2}} (3\sin^2 i' - 2)(2 + 3e'^2)(2 + 3e^2),$$

where

$$\gamma = \frac{\mu'}{\mu} \left(\frac{a}{a'}\right)^3.$$

Taking $\mu' = 132\,712\,440\,041.939\,400\,\mathrm{km}^3\,\mathrm{s}^{-2}$ (Folkner et al. 2014) and the above values for the other parameters, we obtain $\gamma = 0.000\,003\,911\,677$.

Note that, in our analysis, the secular perturbation of M is of no interest, because we determine the semimajor axis and the mean motion from observations independently.

Since, in our solutions, e and i are found to be small, we neglect e^2 and $\sin^2 i$, which are much smaller than unity. The value of the inclination i' of the solar orbit depends on which coordinate system is used. To justifiably neglecting solar perturbations, let us find the maximum value of the secular perturbations putting $\sin i' = 1$. The values for the other parameters are those given above. As a result, we have the following maximum values of secular perturbations:

$$\max \left|\frac{\mathrm{d}\omega}{\mathrm{d}t}\right| = 0.000596 \ \ \mathrm{deg\ day}^{-1},$$

$$\max \left|\frac{\mathrm{d}\Omega}{\mathrm{d}t}\right| = 0.000298 \ \ \mathrm{deg\ day}^{-1},$$

Obviously, compared with the expected amplitudes of the secular perturbations with J_2 terms, secular perturbations with such amplitudes can be neglected.

The attraction of the Sun also results in long-term perturbations in the elements of the satellite orbit. In addition, there are combined perturbations with amplitudes proportional to

$$\gamma J_2 \left(\frac{r_0}{a}\right)^2.$$

To estimate the long-term perturbations from the Sun, we use the formula for the perturbing function derived from that published in Murray & Dermott (2000) and given in Emelyanov & Samorodov (2015). To simplify our estimations, the values of e and e', which are much less than unity, are neglected. Then, the perturbing function is

$$R' = \frac{\mu'}{a'} \left(\frac{a}{a'}\right)^2 \sum_{k=0}^{2} (2 - \delta_{0,k}) \frac{(2-k)!}{(2+k)!} {\sum_{p'=0}^{2}}' F_{2k1}(i) F_{2kp'}(i') \times \cos[(2-2p')u' + k(\Omega' - \Omega)],$$

Table 5. Coefficients of the long-term perturbations from the Sun in the orbital parameters of Linus.

α_0, °	δ_0, °	i °	J_2	K_M °	K_Ω °	Period year
197.616	0.425	2.61	0.0110	5.44670	− 5.33017	85.0228
197.616	0.425	2.61	0.0220	2.72830	− 2.66990	42.5783
197.616	0.425	2.61	0.0345	1.74025	− 1.70299	27.1514
195.532	3.396	1.86	− 0.0345	− 1.78971	1.77012	27.1401
197.616	0.425	2.61	0.1580	0.38100	− 0.37282	5.9286

where the Kronecker symbol $\delta_{0,k} = 1$ if $k = 0$ and 0 if $k \neq 0$ and the prime of the second sum means that the secular term (i.e. the term with $k = 0$ and $p' = 1$) is omitted. Here, $F_{2k1}(i)$ are the inclination functions, while u' and Ω' are the arguments of latitude and longitude of the ascending node of the solar orbit, respectively. Thus, the expression has eight terms, two of which are equal, since $F_{200}(i') = F_{202}(i')$. The formulae for the inclination functions can be taken from Kaula (1966).

Having substituted this expression for the perturbing function into the equations for the elements, after integration, we see that the amplitudes of the long-period terms are proportional to the factors

$$\gamma \frac{n}{k_1\dot{u}' - k_2\dot{\Omega}}, \quad \gamma J_2 \left(\frac{r_0}{a}\right)^2 \left(\frac{n}{k_1\dot{u}' - k_2\dot{\Omega}}\right)^2, \tag{16}$$

where $k_1 = -2$, 0, 2 and $k_2 = 0$, 1, 2. The upper dot denotes a derivative with respect to time.

It follows from (16) that, if $\dot{\Omega} > 0$, there are secular resonances when $\dot{\Omega} = \dot{u}'$ or $\dot{\Omega} = 2\dot{u}'$. If $\dot{\Omega} < 0$, the resonances occur when $\dot{\Omega} = -\dot{u}'$ or $\dot{\Omega} = -2\dot{u}'$. If we take the following values of the parameters (close to the real ones): $\dot{u}' = n' = 0.198\,583\,01$ deg day^{-1}, $a = 1074$ km, $n = 100.155$ deg day^{-1}, $e = 0$, $i = 2°$, $r_0 = 90$ km, we obtain that resonances take place when $J_2 = \pm 0.188$ or $J_2 = \pm 0.376$.

The resonance perturbations are peculiar in that the period of perturbations increases sharply when J_2 approaches its resonance value. The amplitude also increases, since it is proportional to the period.

To estimate the amplitudes of the long-term perturbations in the orbital elements of Linus, we used the calculating program composed earlier to build the theory of motion of Triton (Emelyanov & Samorodov 2015). In this program, we assumed that $e = 0$ and $e' = 0$. Since our goal now is to get approximate estimations of the amplitudes of the long-term perturbations from the Sun, this assumption is also justified in the present study.

Thus, we substituted into the program the values of the parameters of our problem. Several cases were considered, two of them corresponding to two solutions for the satellite orbit. Under the assumptions made ($e = 0$, $e' = 0$), the long-term perturbations appear only in the elements M, i and Ω. Among them, it is the terms in M and Ω with the argument Ω that have maximum amplitudes, approximately equal to each other. The perturbations in the mean longitude are much less, if the inclination of the orbit is much lower.

The program outputs the values of the coefficients K_M and K_Ω in the expressions for the long-term perturbations δM, $\delta\Omega$ in the elements M and Ω, respectively, which have the form

$$\delta M = K_M \sin(\Omega), \quad \delta\Omega = K_\Omega \sin(\Omega).$$

The computed values of the coefficients are presented in Table 5, which gives initial values for the coordinates of the pole of orbit precession, the inclination and J_2. Small variations in other param-

eters do not influence the coefficients significantly. For all cases, we adopted $a = 1074.855\,743$ km, $\mu = 0.508\,129\,859$ km^3 s^{-2}, $n = 100.156\,029\,646$ deg day^{-1}. As for the parameters of the Sun's orbit, the values given above were used.

It is seen from the table that, as J_2 increases from 0.011 to 0.158, the amplitude of the long-term perturbations from the Sun in the longitude of the ascending node decreases from 5.33017° to 0.37282°. The amplitudes of the long-term perturbations from the Sun with other arguments ($k_1 = \pm 2$) are less than those with argument Ω given in Table 5.

The values of the coefficients of long-term solar perturbations obtained show that these perturbations are small compared with the amplitude of the change in the ascending node of the satellite's orbit found from determination of the orbit's pole for a series of dates at the 16.7-yr interval. Thus, unaccounted-for perturbations due to the Sun cannot explain anomalous behaviour of the orbital axis.

Note that, if J_2 becomes smaller, the quantity $\dot{\Omega}$ does not tend to zero. If $J_2 = 0$, there is a secular perturbation in $\dot{\Omega}$ caused by the Sun's attraction. This term has already been considered and estimated.

The next factor in the satellite motion that was neglected is perturbations caused by the J_4 terms in the expansion of the primary's potential function. The secular perturbations caused by this factor are taken into account along with those caused by J_2 terms. As for the long-period perturbations caused by the J_4 terms, they can be determined by the methods of perturbation theory.

We are primarily interested in the changes in Ω. The differential equation for this element has the form

$$\frac{\mathrm{d}\Omega}{\mathrm{d}t} = \frac{1}{na^2\sqrt{1-e^2}\sin i}\frac{\partial R}{\partial i}.$$

The long-period part of the perturbing function containing J_4 terms can be deduced from the common expansion given in Murray & Dermott (2000). Thus, we have

$$R = \mu\frac{1}{a}\left(\frac{r_0}{a}\right)^4 J_4(F_{401}X_0^{-5,2} + F_{403}X_0^{-5,-2})\cos 2\omega.$$

Here, we substitute

$$F_{401} = F_{403} = \frac{5}{32}\sin^2 i(6 - 7\sin^2 i),$$

$$X_0^{-5,2} = X_0^{-5,-2} = \frac{3}{4}\frac{e^2}{(1-e^2)^{7/2}}.$$

As noted above, the inclination i and the eccentricity e are small quantities. Thus, we can also neglect the quantities $\sin^2 i$ and e^2, since they are small compared with unity. As a result, the perturbing function has the form

$$R = \frac{45}{64}\frac{\mu}{a}J_4\left(\frac{r_0}{a}\right)^4 e^2\sin^2 i\cos 2\omega. \quad (17)$$

To obtain the long-period perturbations in Ω, it is necessary to take the differential equation

$$\frac{\mathrm{d}\Omega}{\mathrm{d}t} = \frac{1}{na^2\sqrt{1-e^2}\sin i}\frac{\partial R}{\partial i} + \frac{3}{2}J_2\left(\frac{r_0}{a}\right)^2 n\sin i\delta i, \quad (18)$$

where the second term appears due to the fact that the secular perturbation in Ω depends on i, which, in turn, has long-period perturbations δi. This second term can be neglected, since, as was found during calculations, compared with the first term, it has a factor $\sin^2 i$. Now let us substitute the perturbing function (17) into (18) and integrate this equation over time. First, we obtain the following expression for the first-order long-term perturbation:

$$\delta\Omega = \frac{45}{64}J_4\left(\frac{r_0}{a}\right)^4 e^2\cos i\frac{n}{\dot{\omega}}\sin 2\omega.$$

Then, taking into consideration that

$$\dot{\omega} = \frac{3}{4}J_2\left(\frac{r_0}{a}\right)^2\frac{4 - 5\sin^2 i}{(1-e^2)^{3/2}}n \approx 3J_2\left(\frac{r_0}{a}\right)^2 n,$$

we obtain

$$\delta\Omega = \frac{15}{64}\frac{J_4}{J_2}\left(\frac{r_0}{a}\right)^2 e^2\cos i\sin 2\omega.$$

Using the values of the parameters found earlier in our solutions, the estimated values of $J_2 = 0.158\,545$, $J_4 = -0.062\,056$ and $r_0 = 90$ km, we obtain that the amplitude of the long-period perturbations does not exceed 4.4×10^{-6} degrees.

Thus, it becomes clear that the changes in the longitude of the ascending node Ω found from observations, where the amplitude may reach up to 100°, cannot be explained by unaccounted-for long-term perturbations from the J_4 term.

In our model, we assumed that Linus is a point body. In fact, its non-sphericity can influence its orbital motion. However, we neglect this influence, because the satellite is small in size and there are no data on the parameters of its non-sphericity.

Table 6. Comparison with the results obtained by Vachier et al. (2012). In our article, the 'period' refers to the rate of change of orbital longitude. The semimajor axis is measured in km.

Parameter	Vachier et al. (2012)	This article (Solution 1)
Semimajor axis	1081.5 ± 33.5	1074.8 ± 3.1
Eccentricity	0.006883 ± 0.03124	0.0045 ± 0.0018
Period, days	3.595712 ± 0.000068	3.595693 ± 0.000285
Mass, kg · 10^{-18}	7.75 ± 0.7	7.616 ± 0.072

10 COMPARING THE RESULTS WITH THOSE OF EARLIER STUDIES

The Kalliope–Linus system has been the subject of earlier studies. In addition to attempts to determine the orbit, estimations were made of the shape of Kalliope and orientation of the axis of its gravitational field symmetry. To compare the orbital parameters, we consider one of the most recent studies, the article by Vachier, Berthier & Marchis (2012). It is based on the best set of observations made between 2001 and 2010. However, a fixed Keplerian orbit was used as the model of the satellite's motion. It is claimed in Vachier et al. (2012) that no traces of precession were found either for the line of apsides or for the line of nodes. Since such a model differs significantly from that used in our study, only some parameters can be compared. Table 6 gives the values of these parameters. The comparison shows the coincidence of the results within the limits of the corresponding errors.

After the article by Vachier et al. (2012), a determination of the orbit of Linus was also performed by Sokova et al. (2014). The orbit was found on the basis of nine observed relative positions of the satellite at a 6-day time interval. Since only a few observations were

used in Sokova et al. (2014), we did not compare our results with the results of this work.

Of interest are the results of determining the shape of Kalliope and orientation of its rotation axis from photometric observations published by Descamps et al. (2008). The rotational period of Kalliope turned out to be 4.148 199 hours, so that during one orbital period of the satellite the planet makes 20.8 rotations. Such a period ratio justifies our assumption that the planet has an axisymmetric gravitational field. Descamps et al. (2008) also found the orientation of the planet's rotation axis. For three sets of observations used, three versions of the ecliptic coordinates of the axis were given. The authors also obtained the semiaxes of a triaxial ellipsoid approximating the shape of Kalliope: $a = 117.5$ km, $b = 82$ km, $c = 62$ km. Unfortunately, the article by Descamps et al. (2008) does not provide us with data on the orientation of the axis of Kalliope's body with respect to its rotation axis.

Figs 1, 2 and 3 make it possible to compare the ecliptic coordinates of the axes of rotation obtained in Descamps et al. (2008) with the orbit pole found in the present article from observations. Note that the positions of the planet's axes of rotation are given with an accuracy of about 2°.

As for dynamical oblateness or extension of the planet, the results obtained in Descamps et al. (2008) do not permit any certain conclusions, because there are no data about the position of Kalliope's body with respect to its rotation axis.

The dynamical parameters of the Kalliope–Linus system were also determined by Marchis et al. (2008). The authors claim that they found no precession in the orbit of Linus, assuming that the axis of Linus' orbit coincided with the rotation axis of Kalliope.

11 CONCLUSION

In this study, we tried to build a model of the orbital motion of Kalliope's satellite Linus using all available astrometric obsevations. The impetus for this was the new observations of the satellite made at the Caucasian Mountain Observatory of SAI. The new observations expanded the whole time interval of observations from 10 to 16.7 years. Our plan was to build a model of a uniformly precessing satellite orbit in the time-averaged gravitational field of the fast-rotating Kalliope. For a series of dates distributed into a number of groups, determination of the fixed Keplerian orbit was performed. This determination revealed the type of motion of the orbital axis, which did not correspond to the adopted dynamical model. In the first seven years, the ascending node of the orbit of Linus was moving in a prograde direction, but in the following years it was moving in a retrograde manner. The changes in the node are oscillations with an amplitude of about 100° and a period of about 40 years. Attempts were also made to estimate the influence of the Sun's attraction and the perturbations from the forth harmonics in the expansion of Kalliope's potential function. These effects proved to be too small to explain the unusual behaviour of the satellite's orbital axis. In calculating the perturbations, a problem was set of determining the parameters of the time-averaged gravitational field created by the fast-rotating primary. The body of the primary was modelled as a triaxial ellipsoid rotating around its minor axis. For some pregiven parameters of the triaxial ellipsoid, the coefficients J_2 and J_4 were determined by numerical calculation of the integrals.

For all 121 available relative positions of the satellite, two formal solutions were found for the satellite orbit uniformly precessing around some fixed axis, the coordinates of which were also fitted to observations along with other parameters. The first solution gives a negative value for J_2, which corresponds to a prolate shape of the primary, while the second solution results in positive J_2, corresponding to an oblate body. Both solutions give similar values for the dispersion of the residuals of the satellite's observed positions from those obtained from the model. As the behaviour of the axis found by using separate groups of observations does not agree with the uniform precession model, these two solutions cannot be considered reliable.

As for the satellite's orbital period, semimajor axis and eccentricity, our values for these parameters are very close to those obtained earlier by other authors who used less complete sets of observations.

The results obtained in this article need independent verification by other researchers. For this verification to be correct, the same series of observations that was used in this article should be used. This requirement follows from the strong dependence of the results on the composition of the observations. If some observations are missed, the results could be significantly different. The observations we used can be taken from the ABIN database (Emel'yanov et al. 2018). It is necessary to select observations meticulously to obtain data identical to those used in this article.

ACKNOWLEDGEMENTS

This work was supported by the Russian Foundation for Basic Research, project no. 19-52-15015-CNRS-a, and by the program 'André Mazon' of the Embassy of France in Russia. The development and construction of the speckle polarimeter of the 2.5-m telescope has been funded by the M. V. Lomonosov Moscow State University Program of Development.

REFERENCES

Archinal B. A. et al., 2018, Cel. Mech. Dyn. Astron., 130, 22
Descamps P. et al., 2008, Icarus, 196, 578
Durech J., Sidorin V., Kaasalainen M., 2010, A&A, 513, A46
Emel'yanov N. V., Vashkov'yak S. N., Ural'skaya V. S., 2018, Solar System Research, 52, 260
Emelianov N. V., 1999, Solar System Research, 33, 133
Emelyanov N. V., Samorodov M. Yu., 2015, MNRAS, 454, 2205
Folkner W. M., Williams J. G., Boggs D. H., Park R. S., Kuchynka P., 2014, The Interplanetary Network Progress Report, Jet Propulsion Laboratory, Vol. 42. California Institute of Technology, Passadena, CA, USA, p. 1
Kaula W. M., 1966, Theory of Satellite Geodesy, Applications of Satellitesto Geodesy. Blaisdell, Waltham, MA, p. 124
Marchis F., Descamps P., Hestroffer D., Berthier J., Vachier F., Boccaletti A., de Pater I., Gavel D., 2003, Icarus, 165, 112
Marchis F., Descamps P., Baek M., Harris A. W., Kaasalainen M., Berthier J., Hestroffer D., Vachier F., 2008, Icarus, 196, 97
Margot J. L., Brown M. E., 2003, Science, 300, 1939
Merline W. J., Menard F., Close L., Dumas C., Chapman C. R., Slater D. C., 2001, IAU Circ., 7703, 2
Murray C. D., Dermott S. F., 2000, Solar System Dynamics. Cambridge Univ. Press, Cambridge, p. 608
Safonov B. S., Lysenko P. A., Dodin A. V., 2017, Astron. Lett., 43, 344
Sokova I. A. et al., 2014, Icarus, 236, 157
Soma M., Hayamizu T., Miyashita K., Setoguchi T., Hirose T., 2008, Proc. IAU Symp., 248, 130
Vachier F., Berthier J., Marchis F., 2012, A&A, 543, A68
Viswanathan V., Fienga A., Gastineau M., Laskar J., 2017, INPOP17a Planetary Ephemerides, Vol. 108, Institut de mécanique céleste et de calcul des éphémérides, Paris, France, p. 39

SUPPORTING INFORMATION

Supplementary data are available at *MNRAS* online.

SupplementaryMaterial.txt

Please note: Oxford University Press is not responsible for the content or functionality of any supporting materials supplied by the authors. Any queries (other than missing material) should be directed to the corresponding author for the article.

This paper has been typeset from a TEX/LATEX file prepared by the author.